Helicity Dynamics of Atmospheric Flow

Tan Zhemin (谈哲敏) and *Wu Rongsheng* (伍荣生)
Department of Atmospheric Sciences, Meso-scale Severe Weather Research Laboratory / SEC,
Nanjing University, Nanjing 210008, P. R. China
Received May 18, 1993; revised October 9, 1993

ABSTRACT

Helicity is an important physical variable which is similar to the energy and enstrophy in three-dimensional fluid. It can be used to describe the motion in the direction of fluid rotation and also can be regarded as a new physical variable in turbulence theory. In recent years, it has been used in atmospheric dynamics. In this paper, helicity of atmospheric flow, especially helicity in the boundary layer and in the vicinity of front was discussed. These results show that helicity is usually positive in the boundary layer due to the effect of friction. The helicity of boundary layer flow is larger in anticyclone than that in cyclone, resulting from the different wind structures of boundary layers in anticyclone and cyclone under the geostrophic momentum approximation. It is possible that the helicity is negative at certain height in the baroclinic boundary layer. The influences of nonlinearity and baroclinity on the helicity are important. The so called "Cloud Street" in the boundary layer is related to the dynamics of helicity. Helicity in the atmosphere can be expressed as the temperature advection under some conditions, so helicity would be allowed to describe the frontogenesis and development of frontal structure. The amplitude of helicity increases with time in the frontogenesis. A large gradient of helicity is generated in the region located to the northeast of the surface low and in which the front is formed. In warm frontal region, as well as behind the trough of temperature, the helicity is positive, while the helicity is negative in cold frontal sector and in the ahead ridge of temperature. The largest helicity occurs in the boundary.

Key words: Helicity, Boundary layer flow, Frontogenesis

I. INTRODUCTION

In the study of atmospheric motion, some important physical variables, such as the vorticity that is used to describe the rotation of fluid and the divergence that describes the stretch and constriction of fluid motions have been used to discuss the dynamics of atmospheric motion which includes kinematics and thermodynamics or both of them. In recent years, a new variable, called helicity was introduced in the atmosphere (Etling, 1985; Lilly, 1986; Wu and Tan, 1989; Wu, Lilly and Kerr, 1992). Helicity (strictly speaking helicity density), here denoted by H, is defined as the scalar product of the velocity vector $\vec{V}$ and the vorticity vector $\vec{\omega} = \nabla \wedge \vec{V}$, e.g. $H = \vec{V} \cdot \vec{\omega}$ (Moffat, 1969) which describes the motion in the direction of rotation and is the result of knot for fluid vorticity tube. In isentropic fluid, the helicity is conservative (Moffat, 1969). A great deal of studies for helicity have been carried out in fluid dynamics, magnetohydrodynamics and astrophysics. Helicity is regraded as an important variable equal to the energy and enstrophy for three-dimensional flow. Lilly (1986) suggested that the rotating supercell thunderstorms should be characterized by high helicity and the helicity effects seem to be important in long live storms. Elting (1985) partially discussed the helicity in atmospheric flow and the relationship between the stability of flow and helicity dynamics. Wu and Tan (1989) studied the helicity of atmospheric motion and

indicated that helicity is conservative for quasi-equilibrium flow in geophysical fluid. The relationships between the nonlinear energy transport and helicity of flow in shear thermal convection were discussed by Wu, Lilly and Kerr (1992). In this paper, the importance of helicity in boundary layer and frontogenesis are discussed. These results show that a deep understanding of helicity is rather helpful for dynamics.

In the following sections, the helicity in atmospheric motion is discussed further. The boundary layer flow with the geostrophic momentum approximation, as an example of the application of helicity, is studied in Section III. In Section IV, the helicity dynamics in the atmospheric frontogenesis is researched. The discussion and summary are given in Section V.

II. HELICITY IN THE ATMOSPHERIC MOTION

In the atmospheric motion, the helicity can be expressed as

$$H = \vec{V} \cdot \vec{\omega}. \tag{1}$$

Eq.(1) can be rewritten as

$$H = u\left(\frac{\partial w}{\partial y} - \frac{\partial v}{\partial z}\right) + v\left(\frac{\partial u}{\partial z} - \frac{\partial w}{\partial x}\right) + w\left(\frac{\partial v}{\partial x} - \frac{\partial u}{\partial y}\right). \tag{2}$$

It is convenient to nondimensionalize Eq.(2) with following scale relations:

$$\begin{aligned} (u,v) &= V(u',v'), \quad w = W w', \\ (x,y) &= L(x',y'), \quad z = H_s z', \\ H &= \tilde{H} H', \end{aligned} \tag{3}$$

where $\tilde{H}$, V, W, L, H_s are the characteristic scales of helicity, horizontal velocity, vertical velocity, horizontal length and vertical depth, respectively. The nondimensional variables are noted by primes.

Let

$$\tilde{H} = \frac{V^2}{H_s}, \tag{4}$$

and substitute these scales into Eq. (2), upon dropping the primes, the nondimensional helicity can be expressed as

$$H = u\left(\varepsilon\frac{\partial w}{\partial y} - \frac{\partial v}{\partial z}\right) + v\left(\frac{\partial u}{\partial z} - \varepsilon\frac{\partial w}{\partial x}\right) + \varepsilon w\left(\frac{\partial v}{\partial x} - \frac{\partial u}{\partial y}\right), \tag{5}$$

where $\varepsilon = \lambda_1\lambda_2$, $\lambda_1 = (\frac{W}{V})$, $\lambda_2 = (\frac{H_s}{L})$, ε depends on the ratio of the vertical depth to the horizontal length.

For different scales of atmospheric motions, the helicity can be further simplified.

1) $H_s < L$

In this case, the motion is the large-scale motion or mesoscale motion (e.g. *meso* $-\alpha$, or *meso* $-\beta$ motion).

Let $W = R_o\frac{V}{L}H_s$ or $W = \frac{V}{L}H_s$, then,

$$\varepsilon = R_o(\frac{H_s}{L})^2 \leqslant (\frac{H_s}{L})^2 \ll 1, \tag{6}$$

where $R_o = \frac{V}{fL}$ represents the Rossby number.

So Eq.(5) is approximated by the expression as follows:

$$H \doteq -u\frac{\partial v}{\partial z} + v\frac{\partial u}{\partial z}. \tag{7}$$

For large-scale motion, the helicity in horizontal direction is larger than that in the vertical. For pure two-dimensional shear motion, the helicity can also be written as Eq.(7).

2) $H_s \sim L$

In this case, the motion is a kind of mesoscale motion, $\varepsilon \sim 0(1)$, then Eq.(5) can be rewritten as

$$H = u\left(\frac{\partial w}{\partial y} - \frac{\partial v}{\partial z}\right) + v\left(\frac{\partial u}{\partial z} - \frac{\partial w}{\partial x}\right) + w\left(\frac{\partial v}{\partial x} - \frac{\partial u}{\partial y}\right). \tag{8}$$

For this kind of mesoscale motion, the vertical helicity is as important as the horizontal one.

3) $H_s > L$

This corresponds to small scale motion, $\varepsilon \gg 1$, then Eq.(5) can be rewritten as follows

$$\begin{aligned} H &= \varepsilon u\left(\frac{\partial w}{\partial y} - \frac{1}{\varepsilon}\frac{\partial v}{\partial z}\right) + \varepsilon v\left(-\frac{\partial w}{\partial x} + \frac{1}{\varepsilon}\frac{\partial u}{\partial z}\right) + \varepsilon w\left(\frac{\partial v}{\partial x} - \frac{\partial u}{\partial y}\right) \\ &\approx \varepsilon\left(u\frac{\partial w}{\partial y} - v\frac{\partial w}{\partial x} + w\left(\frac{\partial v}{\partial x} - \frac{\partial u}{\partial y}\right)\right). \end{aligned} \tag{9}$$

Henceforth, we will focus on the problem of large-scale motion. As shown in Eq. (7), it may be written as

$$\begin{aligned} H &= -u\frac{\partial v}{\partial z} + v\frac{\partial u}{\partial z} \\ &= -\vec{k} \cdot \vec{V} \wedge \frac{\partial \vec{V}}{\partial z}, \end{aligned} \tag{10}$$

where $\vec{v} = u\vec{i} + v\vec{j}$, $\vec{i}\ \vec{j}\ \vec{k}$, are the unit vector in the horizontal direction and vertical direction, respectively.

Let $\frac{\partial \vec{V}}{\partial z} = \vec{V}_T$, then Eq. (10) is transformed into

$$H = -\vec{k} \cdot \vec{V} \wedge \vec{V}_T, \tag{11}$$

where $\vec{V}_T$ is the wind shear which determines the sign of helicity.

Eq. (11) indicates that the helicity would vanish if the vertical shear of horizontal wind is parallel to the wind itself in which the wind varies exponentially with height or in the barotropic flow.

For further analysis, Eq. (10) may be rewritten as

$$H = v^2\frac{\partial}{\partial z}\left(\frac{u}{v}\right) = -|\vec{v}|^2\frac{\partial \alpha}{\partial z}, \tag{12}$$

where $\alpha = \alpha(z)$ is the angle between the velocity vector $\vec{v}$ and the velocity component u, i.e., $\tan\alpha = \frac{v}{u}$, $|\vec{v}|^2 = u^2 + v^2$.

Eq.(12) can be used to investigate further the helicity dynamics in shear flow. It is intuitively clear that the helicity is determined completely by the kinetic energy of motion and the variation of the wind vector angle α with height. The sign of helicity only depends on the difference of angle α in vertical direction.

From Eq.(12), we have

$$\begin{aligned} &\frac{\partial \alpha}{\partial z} < 0, \quad H > 0, \\ &\frac{\partial \alpha}{\partial z} = 0, \quad H = 0, \\ &\frac{\partial \alpha}{\partial z} > 0, \quad H < 0. \end{aligned} \tag{13}$$

In shear flow motion, that the wind vector turns counterclockwise with height implies that the helicity of flow is negative. On the contrary, the helicity is positive when the rotation of wind vector is clockwise with height. And the helicity vanishes only when $\frac{\partial \alpha}{\partial z} = 0$, i.e. the angle α is a constant. This case corresponds to an increase or decrease of wind with height without the change of direction.

If $\frac{\partial \vec{V}}{\partial z}$ is replaced by $\frac{\partial \vec{V}_g}{\partial z}$ with the thermal wind balanced equation, then Eq.(11) can be expressed as

$$H = -\left(u\frac{\partial \theta}{\partial x} + v\frac{\partial \theta}{\partial y}\right) = -\vec{V} \cdot \nabla \theta, \tag{14}$$

where θ is the potential temperature.

It shows that the helicity for large-scale flow is related to the temperature advection. If there exists warm air advection, $-\vec{V} \cdot \nabla \theta > 0$, the helicity will be positive, and vise versa. It is obvious that helicity can be taken as a kind of function used to describe the atmospheric frontogenesis.

III. HELICITY IN THE BOUNDARY LAYER

The atmospheric boundary-layer motion is shear flow. Due to the influence of friction, the rotation of wind vector with height is usual clockwise in the boundary layer, i.e., $\frac{\partial \alpha}{\partial z} < 0$, as shown in Fig.1(a), normal Ekman spiral. The helicity is usually positive in the boundary layer.

Wu and Blumen (1982) have ever used the geostrophic momentum approximation (Hoskins, 1975) to study the dynamics of the boundary layer. Their results improved the classical Ekman layer theory and indicated that profiles in cyclone and in anticyclone are different when inertial acceleration term is included. The nondimensional solutions of Ekman layer with the geostrophic momentum approximation can be expressed as

$$\begin{aligned} u &= u_T(1 - e^{-\beta}\cos\beta) - C_1 D^{-2} e^{-\beta}\sin\beta, \\ v &= v_T(1 - e^{-\beta}\cos\beta) - C_2 D^{-2} e^{-\beta}\sin\beta, \end{aligned} \tag{15}$$

where u_T, v_T are velocity at the top of boundary layer in x-axis and y-axis respectively. The parameters β, D, η are:

$$\beta = D\eta,$$
$$D = 1 + R_0\zeta_g,$$
$$\eta = zE^{-1/2}, \tag{16}$$

where R_0 is the Rossby number, E is the Ekman number, ζ_g is the geostrophic relative vorticity of free atmosphere. Details can be found in Wu and Blumen (1982).

Assuming that the nondimensional geopotential height, after Wu and Blumen (1982), is as follows

$$\varphi = \pm(1 - \frac{\alpha_o}{2}r^2)e^{-\frac{\alpha_o}{2}r^2}, \tag{17}$$

where α_o is a positive parameter, r is the distance to the centre. In anticyclone, the positive sign is taken while in cyclone, the negative sign.

With Eq. (17), we have

$$v_g = \frac{\partial\varphi}{\partial r},$$
$$\zeta_g = \frac{v_g}{r} + \frac{\partial v_g}{\partial r}. \tag{18}$$

Substituting (18) into (15), the wind velocity in boundary layer, u, v, are obtained and the helicity of boundary layer flow is given by (5).

In terms of (4), we know that helicity in boundary layer is about $10^{-1}(\mathrm{m}/\mathrm{s}^2)$ which is one order larger than that in the free atmosphere.

Substituting (18) into (15), the wind velocity in boundary layer, u, v, are obtained and the helicity of boundary layer flow is given by (5).

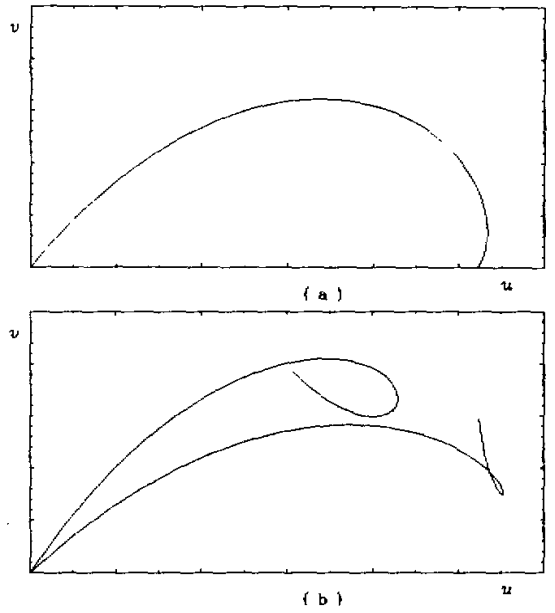

Fig.1. The hodograph in boundary layer, (a) normal barotropic Ekman spiral, (b) baroclinic Ekman spiral (two cases).

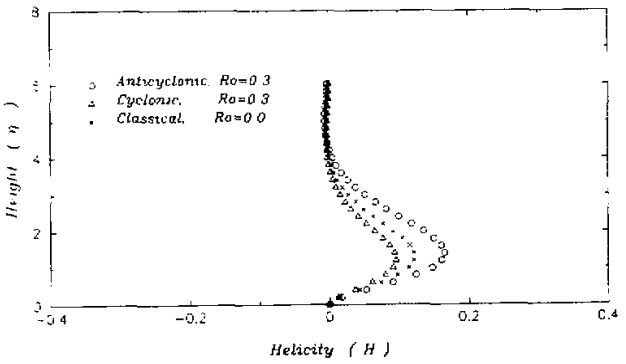

Fig. 2. The distribution of helicity in boundary layer with height at $r = 1.0$ when $\alpha_0 = 0.5$. x: the helicity of classical Ekman flow ($R_0 = 0.0$). o: the helicity of boundary layer under the geostrophic momentum approximation in the anticyclone ($R_0 = 0.3$). Δ: the helicity in cyclone under the geostrophic momentum approximation ($R_0 = 0.3$).

In terms of (4), we know that helicity in boundary layer is about $10^{-1}(\mathrm{m}/\mathrm{s}^2)$ which is one order larger than that in the free atmosphere.

Fig. 2 shows the distribution of helicity with height in the case, $\alpha_0 = 0.5$ and $r = 1.0$, the abscissa is the helicity, and the ordinate is the nondimensional height. Helicity is positive in the boundary layer. As the wind velocity vanishes at lower boundary layer, helicity will reach zero. Helicity increases with the height to its maximum at about 500 m, then decreases with the height to zero at the top of boundary layer where wind shear is zero. On the other hand, due to the different wind structures in boundary layer in different systems under the geostrophic momentum approximation, helicity of flow is larger in anticyclone and smaller in cyclone than that in the classical Ekman flow related to the geostrophic momentum approximation. These results show that the effect of geostrophic momentum on helicity cannot be neglected.

Fig. 3 is the horizontal cross-sections (x, y) of helicity at the height $z = 1.0$, for the anticyclone and cyclone respectively under the approximation of geostrophic momentum when $R_0 = 0.3$, and the classical Ekman flow. The distribution of helicity is axi-symmetric in the boundary layer vortex (either in anticyclone or cyclone). It approaches to zero near the centre of vortex, and increases with the radius of vortex to its maximum at $r = 1.0(r^2 = x^2 + y^2)$, then decreases with increasing r.

In these cases, the three-dimensional spatial distribution of helicity in the boundary layer vortex is two-dimensional ring surface. The dynamics of ring surface depends on the feature of vortex. The fact that helicity is centralized in a limited area may be related to the "cloud street" in the boundary layer which is in agreement with the analysis of Hauf (1985).

In fact, the wind hodographs of boundary layer under the geostrophic momentum approximation, as shown in Wu and Blumen (1982) are similar to the classical Ekman spiral structure (see Fig.1(a)), i.e. $\frac{\partial \alpha}{\partial z} < 0$, the helicity of boundary layer flow under the approximation of geostrophic momentum is positive. This is in agreement with above calculation.

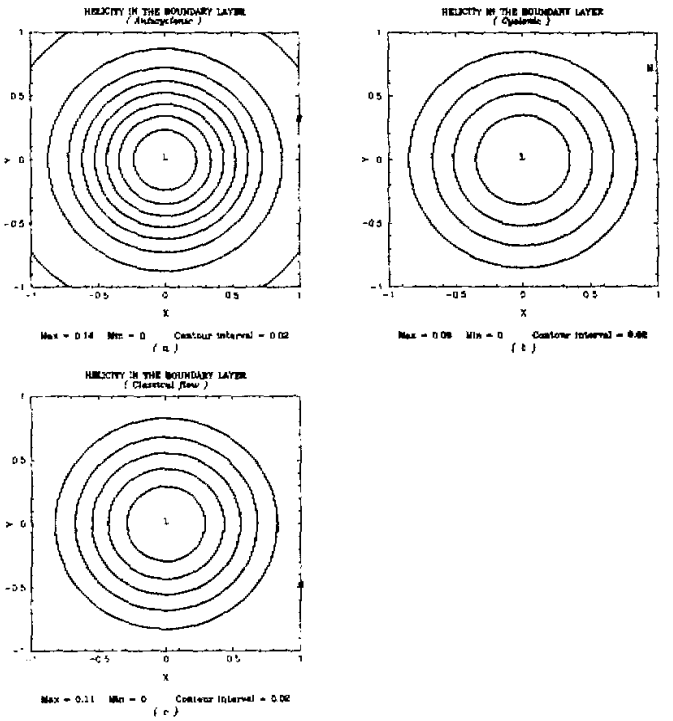

Fig. 3. Horizontal cross-sections of the distributions of helicity in the boundary layer vortex at $z = 1.0$, where $\alpha_o = 0.5$ for, (a) anticyclone ($R_o = 0.3$), (b) cyclone ($R_o = 0.3$) and (c) the classical Ekman flow ($R_o = 0.0$). The contour interval is 0.02.

As to the boundary layer dynamics, the baroclinity contributes greatly to wind velocity. Due to the baroclinic effects, a left hand rotation of wind vector may exist, that is, $\frac{\partial \alpha}{\partial z} > 0$, (see Fig.1(b)), unlike the barotropic boundary layer, the helicity will become negative at certain height in the baroclinic boundary layer. The baroclinic effects are significant for the distribution of helicity in the boundary layer.

In order to understand further the influence of baroclinity on helicity in the boundary layer, the so called average helicity in vertical is defined, denoted by $\overline{H}$. With (12), we have

$$\begin{aligned} \overline{H} &= \frac{1}{H_b}\int_0^{H_b} H dz \\ &\approx -\frac{\overline{|\vec{v}|^2}}{H_b}(\alpha_T - \alpha_o), \end{aligned} \tag{19}$$

where $H_b = \frac{\sqrt{\frac{2K}{f}}}{H_s}$ is the nondimensional depth of boundary layer, $K$is the turbulent eddy coefficient, $\overline{|\vec{v}|^2}$ is the average of $|\vec{v}|^2$ about height. α_T, α_o are the angles of α at the top of boundary layer and at the ground, respectively. $\Delta\alpha = \alpha_T - \alpha_o$ is the total rotation of wind

vector in the whole boundary layer.

With the Ekman theory, assuming that the geostrophic wind linearly varies with height, i.e., $\vec{v}_g = \vec{v}_{go} + \vec{\lambda} z$, the classical baroclinic solution of Ekman layer is obtained easily

$$u = u_{go}(1 - e^{-\eta}\cos\eta) - v_{go}e^{-\eta}\sin\eta + \lambda_x z,$$
$$v = v_{go}e^{-\eta}\sin\eta + v_{go}(1 - e^{-\eta}\cos\eta) + \lambda_y z, \tag{20}$$

where the nondimensional baroclinic parameters $\lambda_x = -E^{1/2}\frac{\partial\theta}{\partial y}$, $\lambda_y = E^{1/2}\frac{\partial\theta}{\partial x}$ are constant, $\vec{\lambda} = \lambda_x \vec{i} + \lambda_y \vec{j}$, $\eta = E^{-1/2}z$, E is the Ekman number. u_{go}, v_{go} are the nondimensional geostrophic winds at the surface of the earth and $\vec{v}_{go} = u_{go}\vec{i} + v_{go}\vec{j}$.

The angle α at the ground, $z = 0$, and at the top of boundary layer, $z = \infty$, are obtained as follows

$$\tan\alpha_o = \left.\frac{v}{u}\right|_{\eta=0} = \frac{(u_{go} - v_{go}) + \lambda_y}{(u_{go} + v_{go}) + \lambda_x}, \tag{21}$$

$$\tan\alpha_T = \left.\frac{v}{u}\right|_{\eta=\infty} = \frac{\lambda_y}{\lambda_x}, \tag{22}$$

hence

$$\tan(\alpha_T - \alpha_o) = \frac{(u_{go} + v_{go})\lambda_y - (u_{go} - v_{go})\lambda_x}{\lambda_x^2 + \lambda_y^2 + (u_{go} + v_{go})\lambda_x + (u_{go} - v_{go})\lambda_y}. \tag{23}$$

In all cases, let us assume that $v_{go} = 0$.

In the barotropic boundary layer, we have $\lambda_y = 0$, $\alpha_o = \frac{\pi}{4}$ and $\alpha_T - \alpha_o = -\frac{\pi}{4}$, so

$$\overline{H} = \frac{4}{\pi}\frac{\overline{|\vec{v}|^2}}{H_b}. \tag{24}$$

The average helicity in the barotropic boundary layer is positive.

In baroclinic boundary layer, if $\lambda_x = \lambda_y$, then $\alpha_o = \alpha_T = \frac{\pi}{4}$ and $\alpha_T - \alpha_o = 0$, thus $\overline{H} = 0$.

If $\lambda_x = 0$, $\lambda_y \neq 0$, with (23) we get

$$\tan(\alpha_T - \alpha_o) = \frac{u_{go}}{\lambda_y + u_{go}}. \tag{25}$$

If $\lambda_y > 0$, then $\alpha_T = \frac{\pi}{2}$, $\tan\alpha_o = 1 + \frac{\lambda y}{u_{go}} > 1$, thus $\alpha_T - \alpha_o > 0$ and $\overline{H} < 0$.

If $\lambda_y < 0$, then $\alpha_T = -\frac{\pi}{2}$, $\tan\alpha_o = 1 - \frac{|\lambda_y|}{u_{go}} < 1$, thus $\alpha_T - \alpha_o < 0$ and $\overline{H} > 0$.

It is clear that the dynamics of helicity in the baroclinic boundary layer which is related to the distribution of potential temperature is more complex than that in the barotropic boundary layer.

IV. HELICITY IN THE VICINITY OF FRONT

Frontogenesis is an important atmospheric process, much work has been done in frontal dynamics. Hoskins (1976), Hoskins and West (1979) have ever applied the approximation of

geostrophic momentum and the geostrophic coordinates to study the nonlinear evolution of an unstable baroclinic Eady wave and frontogenesis. Their results showed that the atmospheric frontogenesis is the result of the nonlinear development of unstable Eady wave.

In the following, the three-dimensional baroclinic Eady wave in steady basic flow with uniform shear in the vertical, as an example, will be used to study the helicity in front.

After Hoskins (1976), the Eady wave motion is assumed to be periodic in horizontal x, and y directions respectively. The fluid motion is bounded by $z = 0$, where the vertical velocities vanish. The basic state of fluid is hydrostatic and geostrophic. The zonal geostrophic flow $\bar{u}(z)$ has an uniform vertical shear simply. The characteristic amplitude of basic flow is U_o.

The evolution equation of baroclinic Eady wave for the perturbation streamfunction Φ in the geostrophic coordinates can be written in nondimensional form as

$$\frac{\partial^2 \Phi}{\partial X^2} + \frac{\partial^2 \Phi}{\partial Y^2} + \frac{\partial^2 \Phi}{\partial Z^2} = 0. \tag{26}$$

The linear boundary conditions are

$$\left(\frac{\partial}{\partial T} + Z\frac{\partial}{\partial X}\right)\Phi_Z - \Phi_X = 0, \quad Z = 0,1, \tag{27}$$

where X,Y,Z are geostrophic coordinates, i.e., $X = x + R_o v_g$, $Y = y - R_o u_g$, $Z = z$, $T = t$. $\Phi = \varphi + R_o \frac{1}{2}(u_g^2 + v_g^2)$, where R_o is the Rossby number. φ is geopotential height, u_g, v_g are geostrophic winds.

The double periodic solution of baroclinic Eady wave is given as

$$\Phi = e^{\sigma T}(a \sin kX' \cosh \kappa Z' + b \cos kX' \sinh \kappa Z') \sin lY, \tag{28}$$

where

$$\begin{aligned} X' &= X - \frac{1}{2}T, \\ Z' &= Z - \frac{1}{2}, \\ \kappa^2 &= k^2 + l^2, \end{aligned} \tag{29}$$

the σ is the wave growth rate, k, and l are the wave numbers in the directions of x, and y respectively, a is the initial wave amplitude, $b / a = 1.502082$.

To most unstable Eady wave mode, we have

$$\sigma = 0.3098\frac{k}{\kappa}. \tag{30}$$

To square Eady wave, $k = 1$. By means of (28), the geostrophic winds are given as follows

$$\begin{aligned} u_g &= -\frac{\partial \Phi}{\partial Y} + U_o Z \\ &= -le^{\sigma T}(a \sin kX' \cosh \kappa Z' + b \cos kX' \sinh \kappa Z') \cos lY + U_o Z, \\ v_g &= \frac{\partial \Phi}{\partial X} \\ &= ke^{\sigma T}(a \cos kX' \cosh \kappa Z' - b \sin kX' \cosh \kappa Z') \sin lY. \end{aligned} \tag{31}$$

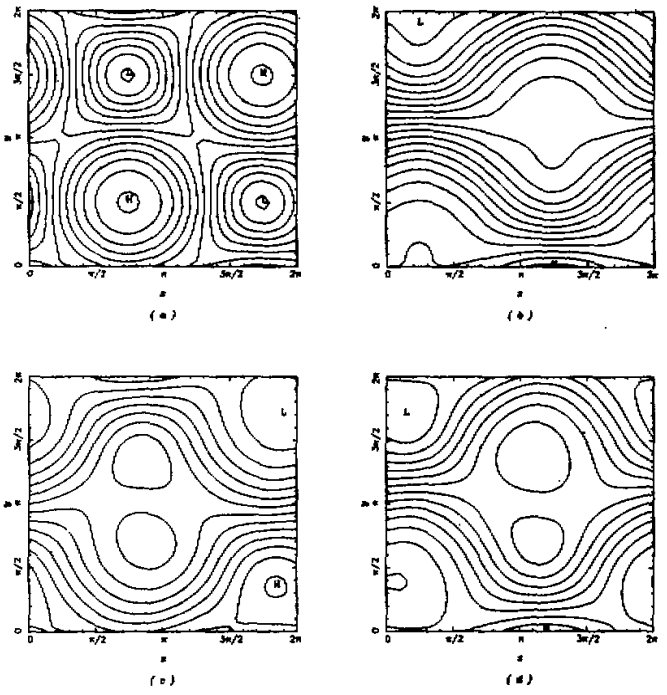

Fig. 4. Horizontal cross-sections of geopotential height and temperature of square Eady wave on the fifth day. (a) and (b) are the contours of geopotenial height at $z=0$, $z=1.0$ respectively, the contour intervals are 0.01 and 0.02 respectively. (c) and (d) are the contours of potential temperature at $z=0.0$ and $z=1.0$ respectively. The contour interval is 0.02.

So the helicity of flow in the frontal zone in geostrophic coordinates is obtained with (17),

$$H_g = -u_g\frac{\partial v_g}{\partial z} + v_g\frac{\partial u_g}{\partial z}, \tag{32}$$

where H_g is the helicity in geostrophic coordinates.

The solutions in geostrophic coordinates have to be converted to physical coordinates in order to get final required solutions. The conversion relationship of geostrophic coordinates and physical coordinates was ever discussed by Wu (1984). Thus, the helicity of flow in physical space can be easily obtained

$$H = \tilde{H}_g + R_o(\tilde{v}_g\frac{\partial \tilde{H}_g}{\partial x} - \tilde{u}_g\frac{\partial \tilde{H}_g}{\partial y}) + O(R_o^2), \tag{33}$$

where

$$\tilde{H}_g = -\tilde{u}_g\frac{\partial \tilde{v}_g}{\partial z} + \tilde{v}_g\frac{\partial \tilde{u}_g}{\partial z}, \tag{34}$$

$$\tilde{u}_g = -le^{\sigma t}(a\sin kx'\cos h\kappa z' + b\cos kx'\sin h\kappa z')\cos ly + U_o z,$$

$$\tilde{v}_g = ke^{\sigma t}(a\cos kx'\cos h\kappa z' - b\sin kx'\sin h\kappa z')\sin ly,$$

and $x' = x - \frac{1}{2}t, \quad z' = z - \frac{1}{2}$.

The distributions of height and potential temperature on the fifth day in the region $0 < x,\ y < 2$ at $z = 0, z = 1.0$ are shown in Fig.4, where $R_o = 0.2,\ a = 0.05$.

In Fig. 4, due to the nonlinear development of unstable Eady wave, there are asymmetric distributions of geopotential height and potential temperature between low and high centres at the surface. The ageostrophic flow results in tight lows and broad highs. The surface low drifts northwards and the high southwards. The growing baroclinic Eady wave transports heat northward. A large temperature wave goes forward northward and northeastward to combine with the lows. A large gradient of potential temperature is also generated, indicating that a frontal zone is formed in this region.

In Fig. 5 (a) and (b), the vertical sections on the fifth day through the line $y = \frac{3\pi}{2}$ which crosses the potential cold front and warm front and along the line $x = \frac{3\pi}{2}$ which includes the warm frontal zone are shown, respectively. Sloping regions of large temperature gradients exist in these sections.

All these results are in common with that discussed by Hoskins (1976).

Fig.6 shows the horizontal sections of helicity in the development of Eady wave at different time and at $z = 0.0$, and $z = 1.0$ respectively.

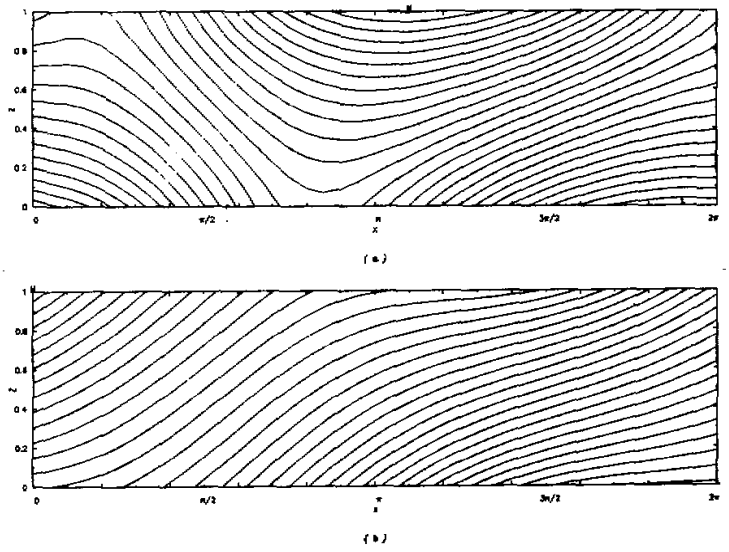

Fig.5. Vertical cross-sections of potential temperature. (a) is the section along $y = \frac{3\pi}{2}$ on the fifth day. The section along $x = \frac{3\pi}{2}$ on the fifth day is shown in (b). Contour interval is 0.01.

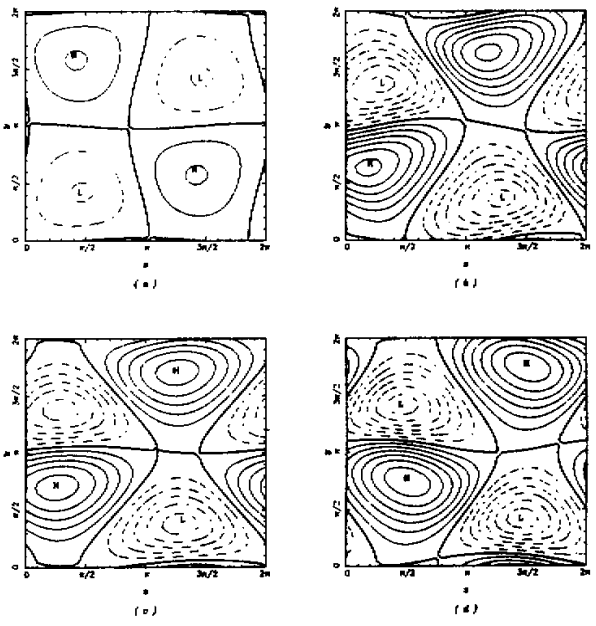

Fig. 6. Horizontal cross-sections of helicity in different time. The bold line indicates the zero line. The positive helicity and negative helicity are indicated by the full and dashed lines respectively. The contour interval is 0.2. In (a), the section on the third day and at $z = 0$ is shown. The sections on the fifth day and at $z = 0$, $z = 0.5$, $z = 1.0$ are shown in (b), (c) and (d) respectively.

Fig.6 indicates that the amplitude of helicity is small and the horizontal distribution of helicity is symmetric at the early stage of development of Eady wave. Due to the unstable growth of Eady wave and ageostrophic effect, the symmetric structure is broken, the positive helicity centres drift northwestwards and the negative centres southwestwards. An asymmetry distribution of helicity is formed. The helicity is concentrated near the centre of the surface low. Then a large gradient zone of helicity occurs, orienting from northwest to southeast in this region, the frontal zone is generated just there. Thus the occurrence of large gradient zone of helicity must be associated with the frontogenesis. The helicity is positive in warm frontal region and negative in cold frontal sector. Since the warm air at the surface is mostly located in cyclonic regions and the cold air in anticyclonic regions, it will be found that the large gradient zone of helicity is just situated near the temperature ridge in the surface and helicity is positive behind the trough of temperature and negative in ahead of temperature ridge. From Fig.4 (a) and (b), it is seen that warm advection occurs behind the trough of temperature, i.e. on the leftside of the surface high centres, the helicity will be positive. Conversely, in the ahead of the trough of temperature exists cold air advection, thus helicity is negative. The horizontal temperature advection is small in the trough or ridge line of temperature, so zero contours of helicity are parallel to the northwestward temperature ridge line and to the northeastward trough line of temperature.

In upper layers, results are similar to those in the lower. The contours of geopotential height are almost parallel to the potential temperature contours. Behind the trough of

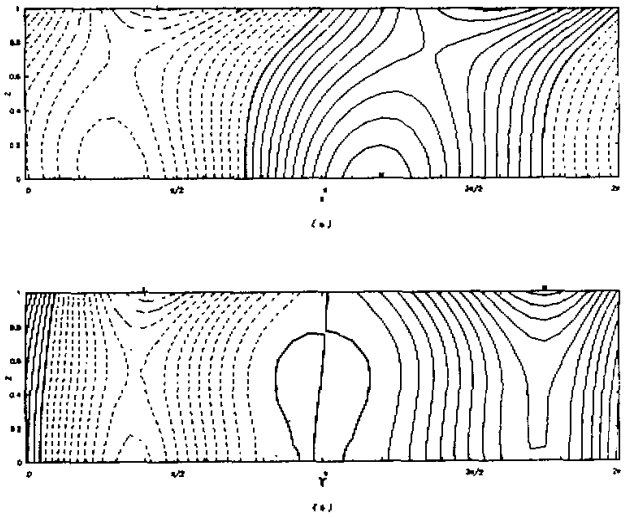

Fig. 7. The same as Fig. 5, but for the helicity, the contour interval is 0.1.

temperature, as well as pressure trough, the helicity is positive, whilst helicity is negative in the ahead of the trough of temperature and pressure. The largest axis of the positive or negative centres of helicity are different in the upper level and in the lower level. The axis turns clockwise with height, which mainly results from the different distributions of wind and temperature in two levels. In mid-level, helicity of flow is smaller than that in the upper and lower level. This is similar to that the frontogenesis is stronger in the boundary than that in the internal area (Hoskins, 1976).

Fig. 7 is the same as Fig. 5, but for the helicity. In Fig. 7(a), the positive helicity sector is mostly in the warm frontal region, but the negative in the cold frontal region. The contours of helicity is tilted to the cold regions. The section in Fig. 7(b) is vertical distribution of helicity along the line $x = \frac{3\pi}{2}$ in which the warm frontal zone is included. The positive helicity is given in the warm sector. The contours of helicity are nearly vertical to the surface in the lower layer. Fig.7 shows that the largest helicity occurs in the boundary due to the largest gradient of temperature generated there.

There is a large vertical shear of flow in the frontal zone. In almost all the warm frontal region, warm advection occupies from the lower level to upper level, wind vector turns clockwise with height, the largest temperature advection appears in the vertical frontal zone. So in the vertical sector of warm front the helicity is almost positive and the large helicity is related to the warm front zone. In cold frontal region, cold temperature advection occurs in most layers, thus helicity is negative. Helicity is an important and interesting variable in atmospheric frontogenesis, which can express the formation of front and describe the new features of front.

As mentioned by Hoskins (1976), the model used here is simple. There is no real or strong cold front formation as the basic zone flow has a uniform vertical shear and zero latitudinal shear. Anyhow the two situations of cold and warm fronts are very similar to those obtained in other frontogenesis models (Hoskins and Bretherton, 1972). The model has been

modified by Hoskins and West (1978). To study helicity dynamics in real atmospheric front is necessary. Maybe to analyse the real observation date about helicity in detail is a best way to study helicity of atmospheric motion.

V. SUMMARY AND CONCLUSION

Helicity is a new physical variable for three-dimensional flow. Helicity is used to study the atmospheric rotation motion. In this paper, the boundary layer flow and frontogenesis, as two examples, have been applied to study the helicity dynamics in the atmosphere. Results show that helicity is almost positive in boundary layer. The influence of nonlinearity and baroclinity on the helicity is significant in boundary layer. Helicity is larger in anticyclone and smaller in cyclone than that in classical Ekman flow with the geostrophic momentum approximation. Negative helicity will be found at the upper level in boundary layer due to the effect of baroclinity. Because of the nonlinear growth of baroclinic Eady wave, heat transports northwards, and large gradient of helicity will be generated in a certain region, most like a frontal region to the north and northeast of the surface lows. Helicity is a new and interesting quantity to describe the frontogenesis. The application of helicity in atmospheric sciences should be studied further in the future.

This project is supported by the National Doctoral Sciences Foundation of China. The authors also acknowledge the support of 'YUMIAO' Science Foundation of Nanjing University.

REFERENCES

Etling, D.(1985), Some aspects of helicity in atmosphere flows, *Beitr. Phys. Atmos.*, **58:** 88–100.

Hauf, Thomas (1985), Rotating clouds with cloud streets, *Beitr. Phys. Atmos.*, **58:** 380–397.

Hoskins, B.J. (1975), The geostrophic momentum approximation and the semi-geostrophic equations, *J. Atmos. Sci.*, **32:** 233–242.

Hoskins, B.J. (1976), Baroclinic Waves and frontogenesis, Part I: Introduction and Eady wave, *Quart. J. Roy. Meteor. Soc.*, **102:** 103–122.

Hoskins, B.J. (1972), Atmospheric frontogenesis models, mathematical formulation and solutions, *J. Atmos. Sci.*, **29:** 11–37.

Hoskins, B.J. and N.V.West (1979), Baroclinic waves and frontogenesis, Part II: Uniform potential vorticity jet flows -cold and warm fronts, *J. Atmos. Sci.*, **36:** 1663–1680.

Lilly, D.K. (1986), The structure, energetics and propagation of rotating convective storms. Part II: Helicity and storm stabilization, *J. Atmos. Sci.*, **43:** 126–140.

Wu, R. (1984), Dynamics of semi-geostrophic flow, *Scientia Sinica* (Ser. B), **XXVII,** 735–743.

Wu, R. and Blumen, W. (1982), An analysis of Ekman boundary layer dynamics incorporating the geostrophic momentum approximation, *J. Atmo. Sci.*, **39:** 1774–1782.

Wu, R. and Tan, Z. (1989), Conservative laws on generalized vorticity and potential vorticity and its application, *Acta Meteor. Sinica*, **47: 437–442** (in Chinese).

Wu, W.S, Lilly, D. K. and Kerr R.M. (1992), Helicity and thermal convection with shear, *J. Atmos. Sci.*, **49:** 1800–1809.